

**ISTANBUL TECHNICAL UNIVERSITY ★ ENERGY INSTITUTE**

**EFFECTS OF NEGLECTED TERMS IN JOSEPHSON JUNCTIONS**



**M.Sc. THESIS**

**Denizhan Ekin ÖNDER**

**Energy Science and Technology Division**

**Energy Science and Technology Programme**

**Thesis Advisor: Prof. Dr. Tahsin T. HAKIOĞLU**

**JUNE 2018**



**ISTANBUL TECHNICAL UNIVERSITY ★ ENERGY INSTITUTE**

**EFFECTS OF NEGLECTED TERMS IN JOSEPHSON JUNCTIONS**



**M.Sc. THESIS**

**Denizhan Ekin ÖNDER  
(301161034)**

**Energy Science and Technology Division**

**Energy Science and Technology Programme**

**Thesis Advisor: Prof. Dr. Tahsin T. HAKIOĞLU**

**JUNE 2018**



**İSTANBUL TEKNİK ÜNİVERSİTESİ ★ ENERJİ ENSTİTÜSÜ**

**JOSEPHSON BAĞLANTILARINDA İHMAL EDİLEN TERİMLERİN  
ETKİLERİ**

**YÜKSEK LİSANS TEZİ**

**Denizhan Ekin ÖNDER  
(301161034)**

**Enerji Bilim ve Teknoloji Anabilim Dalı**

**Enerji Bilim ve Teknoloji Programı**

**Tez Danışmanı: Prof. Dr. Tahsin T. HAKIOĞLU**

**HAZİRAN 2018**



Denizhan Ekin Önder, a M.Sc. student of ITU Institute of Energy student ID 301161034, successfully defended the thesis/dissertation entitled “EFFECTS OF NEGLECTED TERMS IN JOSEPHSON JUNCTIONS” which he prepared after fulfilling the requirements specified in the associated legislations, before the jury whose signatures are below.

**Thesis Advisor :**     **Prof. Dr. Tahsin T. HAKİOĞLU**     .....  
İstanbul Technical University

**Jury Members :**     **Prof. Dr. Fedai İNANIR**     .....  
Yıldız Technical University

**Prof. Dr. İskender A. REYHANCAN**     .....  
İstanbul Technical University

**Date of Submission : 4 May 2018**

**Date of Defense : 7 June 2018**







*To my family,*



## FOREWORD

My main aim for this thesis is bring another aspect to the Josephson junction problems in condensed matter physics. I believe the results are seems unusual and interesting. I would like to thank you to my advisor Prof. Dr. Tahsin T. Hakioglu for his contribution to my physical knowledge and academical life. Also, I want to thank you to my advisor for his support to my personal life.

June 2018

Denizhan Ekin ÖNDER  
Physics Engineer



## TABLE OF CONTENTS

|   | <u>Page</u> |
|---|-------------|
| <b>FOREWORD</b> .....   | <b>ix</b>   |
| <b>TABLE OF CONTENTS</b> .....                                    | <b>xi</b>   |
| <b>ABBREVIATIONS</b> .....  | <b>xiii</b> |
| <b>LIST OF FIGURES</b> .....                                      | <b>xv</b>   |
| <b>SUMMARY</b> .....  | <b>xvii</b> |
| <b>ÖZET</b> .....   | <b>xix</b>  |
| <b>1. INTRODUCTION</b> .....                                      | <b>1</b>    |
| <b>2. SUPERCONDUCTIVITY</b> .....                                 | <b>3</b>    |
| 2.1 Basics of Superconductivity .....                             | 3           |
| 2.2 London Equation .....   | 5           |
| 2.3 Ginzburg Landau Theory .....                                  | 6           |
| 2.4 BCS Theory .....  | 6           |
| 2.1 Type 2 Superconductors .....                                  | 7           |
| <b>3. JOSEPHSON JUNCTIONS AND TUNNELING</b> .....                 | <b>9</b>    |
| 3.1 Current Density .....   | 9           |
| 3.2 Josephson Tunneling .....                                     | 10          |
| <b>4. ANDREEV REFLECTION AND BTK MODEL</b> .....                  | <b>11</b>   |
| 4.1 BTK Model .....   | 11          |
| 4.2 Scattering Matrix Coefficient .....                           | 17          |
| 4.3 Solution of the Andreev Approximation .....                   | 19          |
| 4.4 Andreev Reflection .....                                      | 21          |
| 4.4.1 The ideal interface .....                                   | 21          |
| 4.4.2 Interface with arbitrary transparency .....                 | 23          |
| 4.4 Current and Conductance .....                                 | 24          |
| <b>5. EFFECTS OF NEGLECTED TERMS IN JOSEPHSON JUNCTIONS</b> ..... | <b>27</b>   |
| 5.1 ND Junction.....  | 32          |
| 5.2 DD Junction.....  | 34          |
| <b>6. CONCLUSIONS</b> .....                                       | <b>37</b>   |
| <b>REFERENCES</b> .....   | <b>39</b>   |
| <b>CURRICULUM VITAE</b> .....                                     | <b>42</b>   |



## ABBREVIATIONS

|                      |                                      |
|----------------------|--------------------------------------|
| <b>BCS</b>           | : Bardeen Cooper Schrieffer (theory) |
| <b>BTK</b>           | : Blonder Tinkham Klapwijk (theory)  |
| <b>BdG</b>           | : Bogolubov de Gennes                |
| <b>D</b>             | : D-wave superconductor              |
| <b>GL</b>            | : Ginzburg Landau                    |
| <b>H<sub>c</sub></b> | : Critical Magnetic Field            |
| <b>LB</b>            | : Landauer Büttiker                  |
| <b>N</b>             | : Normal Conductor                   |
| <b>S</b>             | : Superconductor                     |
| <b>T<sub>c</sub></b> | : Critical Temperature               |
| <b>YBCO</b>          | : Lanhtanum Barium Copper Oxide      |





## LIST OF FIGURES

|  | <u>Page</u> |
|--|-------------|
| <b>Figure 2.1</b> : The resistivity drop difference between superconductor and Non-superconductor[4].....  | 3           |
| <b>Figure 2.2</b> : The relation with the critical magnetic field and the temperature [4].....   | 4           |
| <b>Figure 3.1</b> : Josephson junctions and voltage and current relations [6].....   | 10          |
| <b>Figure 4.1</b> : The BTK model for N-S junctions with order parameter [9].....  | 11          |
| <b>Figure 4.2</b> : The Normal (N) side Spectrum [9].....  | 13          |
| <b>Figure 4.3</b> : Superconducting (S) side spectrum [9] .....  | 14          |
| <b>Figure 4.4</b> : The probability coefficients in BTK model for $Z=0$ .....  | 22          |
| <b>Figure 4.5</b> : Reflection and transmission coefficients with increasing barrier strength. ....  | 24          |
| <b>Figure 4.6</b> : Changing of conductance with respect to changing energy and the barrier strength.....  | 26          |
| <b>Figure 5.1</b> : The basic model of ND and DD junctions. Electron and hole reflection and transmission directions are shown .....                 | 27          |
| <b>Figure 5.2</b> : Conductance changing with surface alignments, barrier strength and energy with using fermi approach. Cross terms are zero.....   | 33          |
| <b>Figure 5.3</b> : Conductance changing with surface alignments, barrier strength and energy without fermi approach. Cross terms are not zero ..... | 33          |
| <b>Figure 5.4</b> : Conductance spectrum of two d-wave SC junction with various surface alignments for cross terms equal to zero. ....               | 34          |
| <b>Figure 5.5</b> : Conductance spectrum of two d-wave SC junction with various surface alignments for cross terms not equal to zero .....           | 35          |



## EFFECTS OF NEGLECTED TERMS IN JOSEPHSON JUNCTIONS

### SUMMARY

We show that the existing theory of zero energy Andreev bound state in Josephson junctions with d-wave superconductors neglects a contribution, which under certain conditions drastically changes the appearance of zero bias anomalies. Taking these terms into account allows a better explanation of the experimental data.

It took over 40 years to develop a consistent theory (BCS-Bogoliubov) of superconductivity after its experimental discovery, in the simplest case of spin-singlet, s-wave orbital symmetry. The investigation of other types of symmetry in superconducting and superfluid systems was stimulated after the discovery of A and B phases of  $^3\text{He}$  and unconventional pairings in heavy fermion and cuprate high temperature superconductors (HTS). The non-BCS pairing mechanisms underlying superconducting phases with unconventional symmetry remain one of the most intriguing problems in condensed matter physics. In high temperature superconductors, the pairing symmetry is solidly established as spin-singlet, orbital d-wave, while in different superconductors other symmetries are observed as well. While the nodal lines of the superconducting gap  $d_x^2 - y^2$  attracted much attention, because they allowed as unusual (for BCS case) combination of superconductivity with low-energy excitations, a no less interesting consequence of d-wave symmetry followed from the order parameter changing sign, thus producing an intrinsic, direction-dependent -shift of the superconducting phase. This phenomenon is particularly well manifested in the properties of Josephson junctions with high temperature superconducting materials, leading to the appearance of spontaneous currents and bistabilities, Andreev bound states and zero-bias anomalies in the normal conductance of Josephson junctions produced by the existence of these bound states. The latter was instrumental in establishing their d-wave pairing symmetry and remains the subject of an intensive theoretical and experimental research over the years. The process of Andreev reflection converts the quasi particle current to the supercurrent via the incoming electron-like quasiparticle is being reflected by the off-diagonal superconductor potential (order parameter) as a hole-like quasiparticle and vice versa. The effect takes place not only on SNS junctions but also in weak links and whenever two superconductors with different amplitudes of the order parameter are brought in contact. In Josephson junctions this leads to the formation of Andreev levels. The Andreev reflection amplitude depends on the superconducting phase; therefore, the Andreev levels are phase-sensitive. This allows to express both the superconducting and quasiparticle contributions of the Josephson current in terms of transport through the Andreev levels. The Andreev bound state with energy zero appears in junctions containing a superconductor with direction dependent -phase shift of the order parameter, which leads to canceling the energy-dependent terms in the quantization condition for this level. Its existence produces the specific zero-bias conductance peak (ZBCP) in the differential conductance of the Josephson junction. A convenient method of calculating conductance of restricted quantum structures is based on the

Landauer-Büttiker approach, expressing it through the scattering coefficients. In the following we will show that the appearance of ZBCP in HTS Josephson junctions may drastically change if certain terms, which are usually neglected in such calculations, are properly considered.



# JOSEPHSON BAĞLANTILARINDA İHMAL EDİLEN TERİMLERİN ETKİLERİ

## ÖZET

Bu tezde, d-dalga süperiletken Josephson bağlantılarında var olan sıfır enerji bağlı Andreev durumların var olan teorisinde ihmal edilen terimlerin etkilerini gösterdik. Belirli koşullar altında sıfır tabanlı anomalilerin değişimlerini gösteren bu ihmal edilen terimleri, deneysel verilerle daha iyi bir şekilde karşılaştırılabilmesi için kullandık.

Deneysel keşfinden sonra tutarlı bir (BCS-Bogoliubov) süper iletkenlik teorisi geliştirmek için 40 yıl geçti. Bu teori en basit haliyle Spin-singlet ve s-dalga orbital simetrilerinin temeli atmak için yapıldı. Süper iletken ve süper sıvı sistemlerinde diğer simetri türlerinin araştırılması, 3 He elementinin A ve B fazlarının keşfinden ve ağır fermion ve yüksek sıcaklık süperiletkenlerindeki alışılmamış eşleşmelerden sonra uyarılmıştır.

Konvansiyonel olmayan simetri ile süperiletken fazların altında yatan BCS olmayan eşleştirme mekanizmaları, yoğun madde fiziğinde en ilgi çekici sorunlardan biri olmaya devam etmektedir. Yüksek sıcaklıklı süperiletkenlerde, eşleştirme simetrisi katı bir şekilde spin-singlet, yörüngesel d-dalga olarak kurulurken, farklı süperiletkenlerde diğer simetriteler de gözlemlenir. Düşük enerjili uyarımlarla sıra dışı (BCS durumu için) süperiletkenlik kombinasyonuna izin verdikleri için, Süperiletken boşluk  $dx^2-y^2$ 'nin düğüm çizgileri çok dikkat çekerken, d-dalgası simetrisinin daha az ilginç bir sonucu olan düzen parametresi, değiştirme işaretinden takip edilir, böylece içsel bir sonuç elde edilir. Böylece süper-iletken fazın içsel, yön-bağımlı-kayması üretilir. Bu fenomen, yüksek sıcaklıktaki süper iletken malzemelerle Josephson bağlantılarının özelliklerinde özellikle iyi bir şekilde kendini gösterir. Andreev bağlı durumları bu bağlı durumların varlığından kaynaklanan Josephson bağlantılarının normal iletkenliğindeki durumları ve sıfır tabanlı anomalilerini gösterir. İkincisi, d-dalgası eşleştirme simetrisini oluştururken etkiliydi ve yıllar boyunca yoğun bir teorik ve deneysel araştırmanın konusu olmaya devam ediyordu.

Andreev yansıması süreci, kuazi-parçacık akımını süper akıma dönüştürür. Bu işlem gelen elektron benzeri kuazi-parçacığın süperiletken potansiyelinin diyagonal olmayan kısmından delik benzeri kuazi-parçacık olarak yansımasıyla olur. Bu işlem aynı zamanda tersinirdir. Yani delik benzeri parçacık aynı şekilde süperiletken potansiyelinin diyagonal olmayan kısmıyla etkileşerek electron benzeri kuazi-parçacığa dönüşür. Josephson kesişimlerinde temel akım prensibi bu şekildedir. Burada süperiletkenin potansiyelinin açısına bağlı olarak kesişim noktasında akımda artış ve azalma gözlemlenir.

Bu tezde yapılan çalışma, bu yüzey açılarının ve bağlantı noktasına konulan bir potansiyel bariyerin değerinin değişimiyle akımda olan değişimleri gözlemlemeye çalışmaktır. Etki sadece SNS (süperiletken-normal-süperiletken) bağlantı noktalarında değil, aynı zamanda zayıf bağlantılarda ve düzen parametresinin farklı genliklerine sahip iki süperiletken ile temasta bulunur. Bu durum Josephson bağlantı noktalarında

Andreev seviyelerinin oluşmasına yol açar. Andreev yansıma genliği süperiletkenin fazına bağlıdır. Bu nedenle Andreev seviyeleri faza duyarlıdır. Bu, Josephson akımının Andreev seviyeleri aracılığıyla taşınması açısından süperiletken ve kuazi-parçacık katkılarını ifade etmeyi sağlar.

Josephson bağlantı noktalarında sıfır enerji Andreev bağlı durumu yöne bağlı süperiletken durumunu gösterir. Bu ayrıca düzen parametresinin (süperiletkenin potansiyel fonksiyonu) faz kaymasını gösterir. Bu durumun varlığı, Josephson bağlantı noktalarının diferansiyel iletkenliğinde spesifik bir sıfır öngerilim iletkenlik tepe noktasını üretir. Kısıtlı kuantum yapıların iletkenliğinin hesaplanması için uygun bir yöntem olan Landauer-Büttiker yaklaşımı uygulanmaktadır. Tez içerisinde Bölüm 4.5 içerisinde bu modelin akım ve iletkenlik için üretilen matematiksel modeline değinilmiştir. Bu model, Andreev hesaplarından gelen Andreev yansıma, normal yansıma, elektron benzeri geçiş ve delik benzeri geçiş olasılık sabitlerinin ve akım korunumundan çıkan kuazi-parçacık düzeltme denklemlerinin kullanılması ile bize akımın ve iletkenliğin, yansıma ve geçiş olasılık sabitleriyle nasıl bağlantılı olduğunu gösterir. Bu model saçılma katsayıları ile ifade edilir.

Bu tezde, belirli şartların uygun bir şekilde dikkate alınması durumunda Josephson kavşaklarında sıfır öngerilimli iletkenlik tepe noktasının ortaya çıkmasının ciddi şekilde değişebileceğini göstereceğiz. Bölüm 5'te özellikle DD süperiletken Josephson kesişim noktalarında bu sıfır öngerilimli iletkenlik tepe noktalarının değişen parametrelerle klasik modelden ayrıldığını inceleyeceğiz.

Genel olarak klasik modellerde (BTK), Josephson bağlantı noktalarının matematik modelleri yazılırken, dalga vektörleri ve momentumlar hesaplarda kolaylık olması sebebiyle fermi seviyesinde kabul edilir. Bu fermi yaklaşımı, bağlantı noktasının tüm noktalarında düzlemsel eksene göre hareket eden parçacıkların momentumlarını eşit almayı öngörür. Fakat kullanılan süperiletkenlerin düzen parametre fonksiyonlarının yine düzlemsel eksene göre yaptıkları açılarının farkına göre, gelen, yansıyan ve geçen parçacıkların momentumlarının eşit olması prensibi, iletkenlik hesaplarında bazı detayların gözükmemesine yol açar.

Biz bu tezde gönderilen elektronu düzlemsel eksene paralel olacak şekilde göndererek, süperiletkenin düzen parametre fonksiyonunun düzlemsel eksen ile yaptığı açığı değiştirerek iletkenlik üzerine etkisini inceledik. D-dalga süperiletkenlerinin yapısından dolayı 45 derecelik değişimler ile gelen parçacığın bağlantı noktasında nasıl bir potansiye ile karşılaşabileceğini öngörebiliyoruz. Burada beklenen sonuç, enerjinin sıfıra gitmesiyle sıfır öngerilimli iletkenlik tepe noktasının sonsuza gitmesidir. Hesaplarda D-dalga Josephson bağlantılarında bu durum görülmektedir.

Hesapların daha anlaşılır ve kolay olabilmesi için iki d-dalga süperiletkenin Josephson bağlantı noktasında malzeme özelliklerini aynı aldık. Bu durumda düzel parametresinin katsayıları yani potansiyellerin genlikleri iki taraf içinde eşit değerde alınarak sadece yüzey açılarının ve bağlantı noktasında alınan yalıtkan potansiyel bariyerin değişiminin etkisini gözlemlemeyi hedefledik. Buna ek olarak normal metal ve süperiletken Josephson bağlantı hesaplarında normal metalin düzen parametresi olmadığı için, delta potansiyel fonksiyonu sıfıra eşit olmaktadır. Burada ilginç olan, bölüm 5'te de görüneceği üzere, ihmal edilen terimlerin hesaba katılmasıyla üretilen algoritmada fermi yaklaşımının yapıldığı değerlerde sonuçların klasik BTK modeline benzemesidir. Yaklaşımın yapılmadığı şekillerde ise beklenmeyen bir takım ilgi çekici sonuçlar elde edilmektedir. Daha önce bu hesapların denendiği bir araştırma bulunmadığı için, bu tez teorik olarak bir model öngörüsü ortaya koymaktadır. Ayrıca

hesapların basitleştirilmesi için, Spin-yörünge çifti etkisinde hesaplara dahil edilmemiştir. Bu durum, spin etkileşiminin olmadığını ve gelen, yansıyan ve geçen parçacıkların spin yönlerinin aynı kalmasını öngörür. Böylece hem sistemin Hamilton matrisinin boyutu yarıya inmiş, hemde iki taraf arasında spin değişiminden kaynaklanabilecek diğer etkiler grafiklere konulmamıştır. Bu durum sayesinde, sadece yüzey açısı parametrelerinin ve yalıtkan bariyer genliğinin iletkenlik üzerinde ki etkisi incelenebilmiştir.







## 1. INTRODUCTION

The first successful try in superconductivity was made by Heike Kamerlingh Onnes in liquefying helium in 1908. He tried to make a research about electrical resistivity of metals at low temperatures. The first experiments are done on mercury because of its purity. The resistance started to decrease while temperature decreased. After the temperature reached to 4.2 K, the resistance showed a sharp drop to zero. On the other hand, with increasing the temperature, resistance acted like reverse. After this interesting behavior of mercury investigated, similar experiments were tried on lead and tin. Lead's resistivity showed to same drop at 7.2K and tin's resistivity showed at 3.7K. After this result, the temperatures where the resistivity drop zero called critical temperatures. Therefore, this effect named as superconductivity. The discovery of the liquefaction of helium and superconductivity term brought 1931 Nobel Prize to Onnes. Onnes also discovered the magnetic field's destruction effect on superconductivity. According to his research, after a specific magnetic field strength for each material, the superconductivity disappears. This specific value is also called critical magnetic field ( $H_c$ ) [1].

Another important effect in superconductivity is called Meissner effect. W. Meissner and R. Oschenfield showed that a superconductor gave a permission for up to a specific magnetic field inside itself. Therefore, to specify a materials superconducting property resistance drop and the Meissner effect must be observed below its critical temperature.

The formulation of superconductivity is created by Fritz and Heinz London in 1935 and its called the London Theory [2]. This theory brought the idea of order parameter and coherence length.

One of the most popular superconducting theory is called BCS theory in 1957. The theory got its name from the scientist Bardeen, Cooper and Schrieffer. The basic idea in this theory was developing a superconducting model which includes all parameters of superconductivity.

Different from low temperature superconductivity, the theory of high critical temperature superconductivity is discovered by Alex Müller and George Bednorz in 1986. The experiments showed that a lanthanum-barium-copper-oxide (YBCO) showed superconducting behavior at 30K [3]. In addition of this high temperature superconductivity, Wu et al showed that yttrium-barium-copper-oxide transition temperature was 93K. This result was interesting because the temperature of 93K is higher than the boiling point of liquid nitrogen which is 77K. In that case, YBCO is a very popular superconductor today.

In this thesis, we focused on a theory of multi superconducting junctions separated with a thin insulating layer. These junctions called as Josephson Junctions. In Chapter 2, we showed some classical properties and theories of superconductivity. In Chapter 3, we derived some important equations of Josephson Junctions to understand the cooper pairs, current behavior, flux quantization and the tunneling phenomena. In Chapter 4, we derived the Classical Andreev Reflection calculations to understand the model we used. The main model is called Blonder, Tinkham, Klapwijk (BTK) which is a model of unconventional superconducting junctions. We derived the conductance results of this BTK model. In Chapter 5, we tried to understand effects of neglected terms in these unconventional Josephson junctions to make a general model which is never done before.

## 2. SUPERCONDUCTIVITY

In this Chapter, we tried to have a look of basic properties and equations of Superconductivity. To understand how Superconductivity works, one need to know basics of Superconductivity.

### 2.1. Basics of Superconductivity

The superconductors mainly divided into two; perfect conductivity and perfect diamagnetism. The resistivity is decreased with the decreasing temperature because of the electron and phonon scattering. However, in superconductors the sharp drop of resistivity to zero at a specific temperature called transition temperature. The main aspect of superconductors is the conductivity becomes perfect under these transition temperatures.

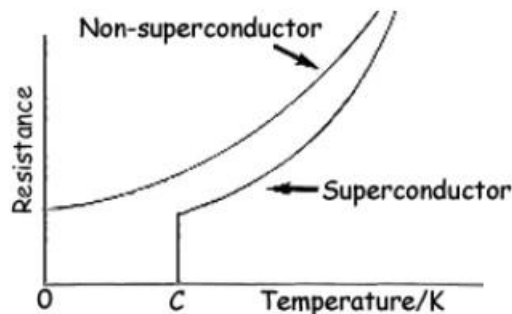


**Figure 2.1:** The resistivity drop difference between superconductor and Non-superconductor.

As seen in the Figure 2.1 resistivity drops to zero suddenly while the temperature decreasing in a superconductor. This perfect conductivity can have destroyed using magnetic field. As mentioned in the Chapter 1, the applying external magnetic field can destroy the superconductivity. If an external magnetic field applied to a superconductor for a while and then removed, there will be an induced current starts to flow around superconductivity continuously. This induced current creates induced

magnetic flux. The magnetic flux seen in the superconducting ring is quantized. This means it can only have integer values. This is called magnetic flux quantum.

The destruction of superconductivity with applying magnetic field process is similar as temperature and resistivity curve. If the applying magnetic field excess the critical magnetic field ( $H_c$ ), then the material lost its superconducting property. On the other hand, critical magnetic field is a function of temperature. The critical magnetic field equation is given in the Equation (2.1).

$$H_c(T) = H_c(0)[1 - (\frac{T}{T_c})^2] \tag{2.1}$$

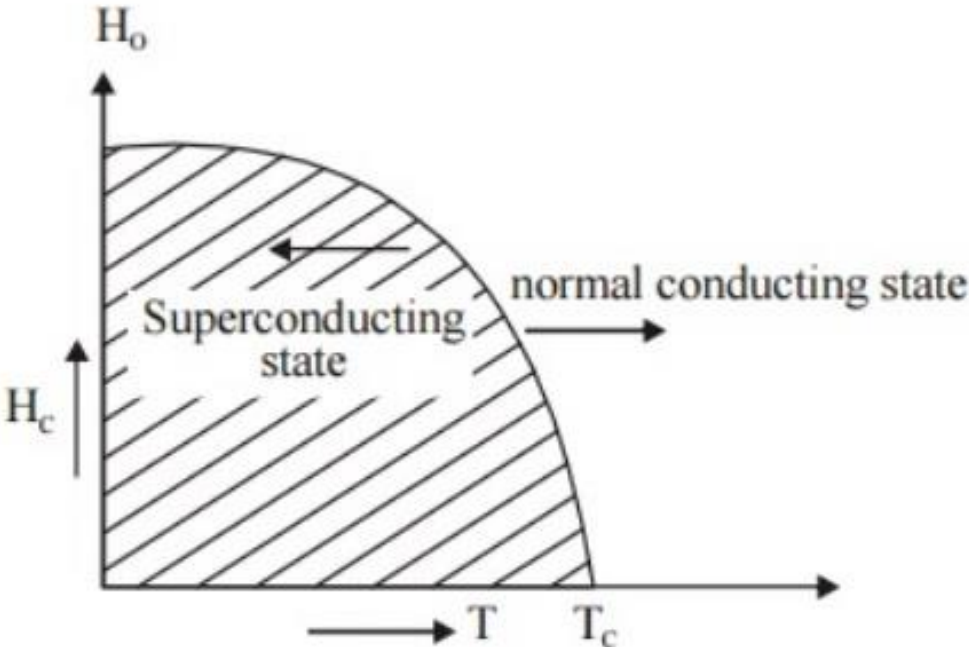


**Figure 2.2:** The relation with the critical magnetic field and the temperature [4].

As we can see in the Figure (2.2) the superconductivity depends on both a critical magnetic field and a critical temperature.

The diamagnetic properties of superconductors also a well-known situation. This property is differing the superconductors from ideal conductors. These superconducting states of the materials creates opposite induced magnetic field if any external magnetic field applied. This induced field is created from the induced current which is created by applying external field. This phenomenon is called Meissner effect [5].

## 2.2. London Equation

The London equations are basic calculations for showing the superconducting phenomena.

$$m \frac{dv}{dt} = eE - \frac{mv}{\tau} \quad (2.2)$$

The London formulations is starts with the electrical conductivity in Drude model seen in the Equation (2.2). In here,  $v$  is the average velocity of electrons,  $m$  refers to mass of the electrons,  $e$  is charge of an electron,  $E$  is energy and  $\tau$  is mean time between scattering of electrons. In the superconducting state, the assumption is telling us there is no scattering between electrons. Therefore, the mean time dependent side goes to zero in the Equation (2.2) and we got a new derivation below;

$$m \frac{dv}{dt} = eE \quad (2.3)$$

To deriving the London equation, first need to write superconducting current density;

$$J_s = n_s e v_s \quad (2.4)$$

In the Equation (2.4) the  $n_s$  and  $v_s$  terms are electron density and average velocity of electrons respectively. With combining the Equation (2.4) and (2.3) we get

$$E = \frac{d}{dt} \left[ \frac{m}{n_s e^2} j_s \right] \quad (2.5)$$

$$E = \frac{d}{dt} (\Lambda j_s) \quad (2.6)$$

$$\Lambda = \frac{m}{n_s e^2} \quad (2.7)$$

In here the Equation (2.6) is refers to first London equation. The second London equation is derived from Ampere's Law

$$-\nabla^2 H = \nabla \times J \quad (2.8)$$

Combining Equation (2.8) with (2.6) and we get the equation below

$$-\nabla^2 \frac{\partial H}{\partial T} = \nabla \times E \cdot \frac{1}{\Lambda} \quad (2.9)$$

Applying Maxwell Faraday equation to Equation (2.9) we get the equation below

$$-\nabla^2 \frac{\partial H}{\partial T} = -\frac{\partial H}{\partial t} \cdot \frac{1}{\Lambda} \quad (2.10)$$

The field equation in Equation (2.10) gives

$$\nabla \times J = \frac{-B}{\Lambda} \quad (2.11)$$

The Equation (2.11) is also known as second London Equation. The solution of the second London equation also gives the penetration depth which is stated in Equation (2.12) below

$$\lambda = \sqrt{\frac{\Lambda}{\mu_0}} \quad (2.12)$$

The penetration depth stating in the Equation (2.12) shows how much magnetic field penetrate inside a superconductor [6].

### 2.3. Ginzburg Landau Theory

The main reason of this model is also to formulating the superconductivity phenomena. In this approach, quantum mechanical descriptions are using. The idea is the showing long range coherently electrons with wave function. Also, the density of electrons written from the absolute square of this distance dependent wavefunction.

The theory is also shows the Coherence length which is a characteristic length of superconductors as a function of temperature. In addition, the Ginzburg-Landau parameter usually used to describe to type of the superconductor. For Type 1 superconductors the Ginzburg-Landau parameter is lower than 1 [7].

### 2.4. BCS Theory

The BCS theory mainly answers the question of why superconducting electrons do not face with any resistance below their transition temperature. This theory usually used for understanding the physics of superconductors.

BCS theory begins with the cooper pair formations below critical temperatures. Phonon-electron interaction causes attractive forces and bound two electrons which is defined as cooper pairs. To stabilize the spin conservation to be zero, these electrons have opposite spins. This shows us the bosonic structure of cooper pairs. In the low

temperatures, an electron create phonon where another electron absorbs that phonon the cooper pairs are started to form [5].

## **2.5. Type 2 Superconductors**

This type of superconductors are found by Abrikosov. His theory depends on different behaviors of some superconductors under a magnetic field. In this type, some superconductors still preserve its superconducting behavior if external magnetic field exceeds the critical magnetic field. Type 2 superconductors have two critical magnetic field. Also, the Ginzburg-Landau parameter is greater than one in these superconductors.

In type 2 superconductors, the applied magnetic field penetrates the material. This magnetic field vectors formed as vortices inside the material. After exceeding the first critical magnetic field value, the material still preserves its superconducting behavior. However, with increasing the vortices size, in the second critical magnetic field these vortices cross each other and destroy the superconductivity [5].





### 3. JOSEPHSON JUNCTIONS AND TUNNELING

The Josephson Junction is a junction between two superconductors. The cross section of these two superconductors is made by an insulating layer. This phenomenon is depending on electron tunneling in these junctions. With the tunneling of these electrons, the supercurrent is created. This model is using in many quantum devices. At low temperatures, the lattice vibrations of crystals are very small. Two electrons can move with pairing by attracting the lattice. These pairs are Cooper pairs and they can move without resistivity in superconductors [8]. The Schrödinger's wave function represents these pairing electrons [6]. The pairing has a twice mass of an electron and half density.

The representative wave function is giving in the Equation (3.1).

$$\psi(r,t) = \sqrt{n(r,t)} e^{i\theta(r,t)} \quad (3.1)$$

#### 3.1. Current Density

The current density expression with wavefunction is seen in the Equation (3.2) and the superconducting current density equation depends on magnetic vector potential "A" is showing in the Equation (3.3) below

$$J_s = q^* \operatorname{Re} \left\{ \psi^* \left( \frac{\hbar}{im} \nabla - \frac{q^*}{m^*} A \right) \right\} \quad (3.2)$$

$$J_s = q^* n^*(r,t) \left( \frac{\hbar}{im^*} \nabla \theta(r,t) - \frac{q^*}{m^*} A(r,t) \right) \quad (3.3)$$

We can use gauge transformations for vector and scalar potential showing in the Equation (3.4) and (3.5) respectively

$$A' = A + \nabla \chi \quad (3.4)$$

$$\Phi' = \Phi + \frac{\partial \chi}{\partial t} \quad (3.5)$$

The new phase is stated in Equation (3.6).

$$\theta' = \theta + \frac{q^*}{\hbar} \chi \quad (3.6)$$

The new current density with using gauge transformation is shown in the Equation (3.7) [6].

$$J_s = q^* n^*(r,t) \left( \frac{\hbar}{m^*} \nabla \theta'(r,t) - \frac{q^*}{m^*} A'(r,t) \right) \quad (3.7)$$

### 3.2. Josephson Tunneling

The Josephson junction model and the mathematical representations are shown in the Figure (3.1).

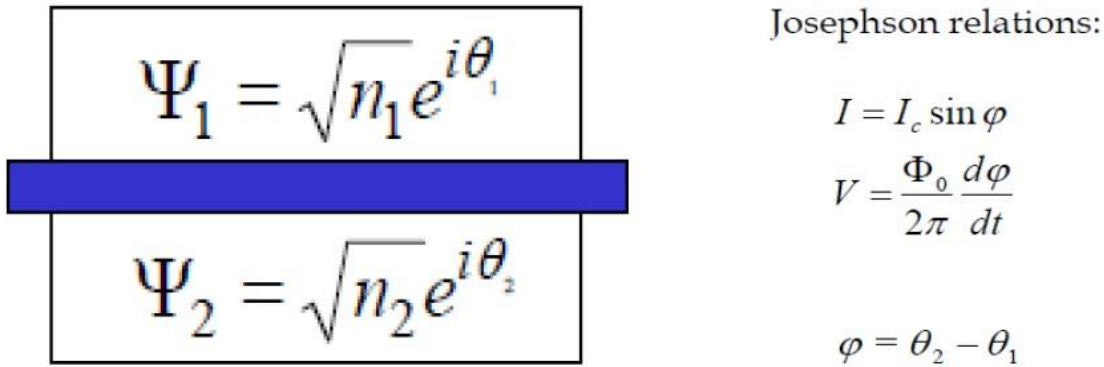


**Figure 3.1:** Josephson junctions and voltage and current relations [6]

In the model, each superconducting region is showing with their own wavefunctions. The tunneling effect occurs in the thin insulator layer showing in blue color in the Figure (3.1). We do not need to solve this tunneling phenomena in this part. We solved this model in the Andreev reflection and BTK model in Chapter 4 and 5.

## 4. ANDREEV REFLECTION AND BTK MODEL

### 4.1. BTK Model

We used Normal metal and Superconductor junction in the first aspect. The general model and the gap order parameter delta is shown in the Figure (4.1).

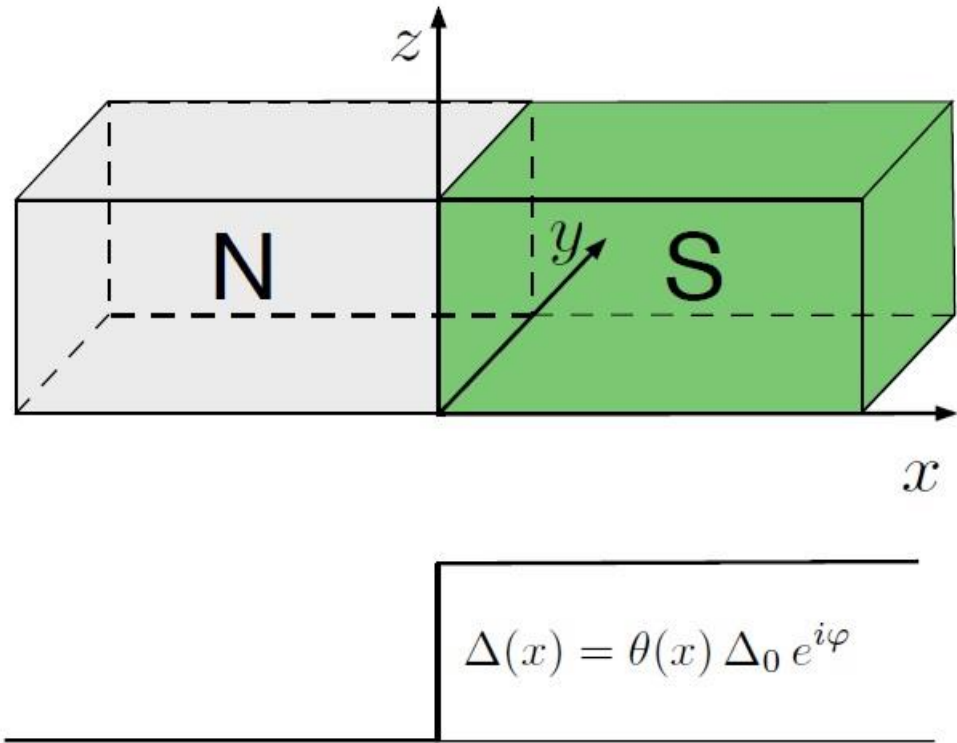


**Figure 4.1:** The BTK model for N-S junctions with order parameter [9].

In the model shown in the Figure (4.1) the three-dimensional coordinates are  $x$  (longitudinal),  $y$  and  $z$  (transversal). For the simplicity of the calculations, we put the junction in the origin where  $x$  is equal to zero. We can write the system with using the Bogolubov de Gennes Equation showing in the Equation (4.1) [9].

$$\begin{pmatrix} H_e & \Delta \\ \Delta^* & -H_e^* \end{pmatrix} \begin{pmatrix} u \\ v \end{pmatrix} = E \begin{pmatrix} u \\ v \end{pmatrix} \quad (4.1)$$

The step like junction order parameter is showing in the Equation (4.2).

$$\Delta(x) = \theta(x)\Delta_0 e^{i\varphi} \quad (4.2)$$

According to three dimensional coordinates, we can separate the wavefunction into transversal and longitudinal parts showing in the Equation (4.3).

$$\Psi(x, y, z) = \psi(x)\Phi_n(y, z) \quad (4.3)$$

In the function includes transverse coordinates (y, z) the letter “n” donates the quantum number. We wrote the Schrödinger’s equation of the system in Equation (4.4) with transversal energy and potential.

$$\left[ \frac{\hbar^2}{2m} \left( \frac{\partial^2}{\partial x^2} + \frac{\partial^2}{\partial y^2} \right) + V_{\perp}(y, z) \right] \Phi_n(y, z) = E_n \Phi_n(y, z) \quad (4.4)$$

The energy is equals to sum of both transversal and longitudinal energies showing in the Equation (4.5).

$$E = E_{\parallel} + E_n \quad (4.5)$$

For a given mode “n”, the effective chemical potentials can be derived showing in the Equation (4.6).

$$\varepsilon_{Fn} = \varepsilon_F - E_n \quad (4.6)$$

The assumption that  $\varepsilon_F$  has already includes the self-consistent potential U.

After that, we put a Dirac potential barrier at the boundary to with a strength to show the contact resistance. With Using the Equations below, the final Hamiltonian from BdG is showing in the Equation (4.7) [10].

$$\begin{pmatrix} -\frac{\hbar^2}{2m} \frac{\partial^2}{\partial x^2} - \varepsilon_{Fn} + \Lambda \delta(x) & \Delta(x) \\ \Delta^*(x) & +\frac{\hbar^2}{2m} \frac{\partial^2}{\partial x^2} + \varepsilon_{Fn} - \Lambda \delta(x) \end{pmatrix} \begin{pmatrix} u(x) \\ v(x) \end{pmatrix} = E \begin{pmatrix} u(x) \\ v(x) \end{pmatrix} \quad (4.7)$$

The equation stated in Equation (4.7) is called BTK (Blonder-Tinkham-Klapwijk) model. The first aim is to find solutions with non-negative energies.

Lets look up for Normal (N) side solutions where order parameter goes to zero as seen in the Equation (4.8).

$$\begin{pmatrix} -\frac{\hbar^2}{2m} \frac{\partial^2}{\partial x^2} - \varepsilon_{Fn} & 0 \\ 0 & +\frac{\hbar^2}{2m} \frac{\partial^2}{\partial x^2} + \varepsilon_{Fn} \end{pmatrix} \begin{pmatrix} u(x) \\ v(x) \end{pmatrix} = E \begin{pmatrix} u(x) \\ v(x) \end{pmatrix} \quad (4.8)$$

From the N side equation, we can see two particle and hole solutions stated in the Equations (4.9) and (4.10) respectively

$$\Psi_{\pm}^e(x) = \begin{pmatrix} 1 \\ 0 \end{pmatrix} e^{\pm ik_e x} \quad (4.9)$$

$$\Psi_{\pm}^h(x) = \begin{pmatrix} 0 \\ 1 \end{pmatrix} e^{\pm ik_h x} \quad (4.10)$$

Where

$$k_e = k_{Fn} \sqrt{1 + \frac{E}{\varepsilon_{Fn}}} \quad (4.11)$$

$$k_h = k_{Fn} \sqrt{1 - \frac{E}{\varepsilon_{Fn}}} \quad (4.12)$$

$$k_{Fn} = \frac{\sqrt{2m\varepsilon_{Fn}}}{\hbar} \quad (4.13)$$

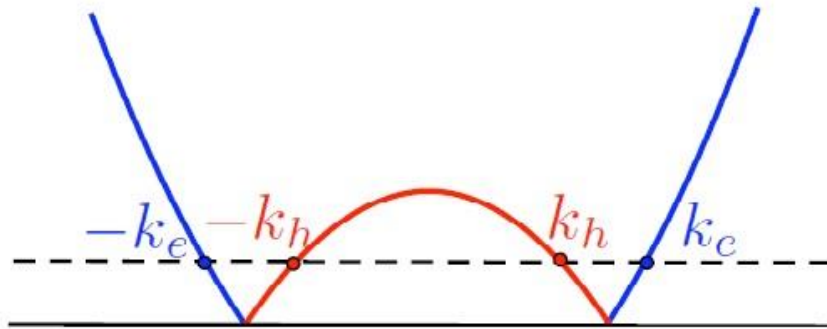


**Figure 4.2:** The Normal (N) side Spectrum [9].

After we reached the solutions of the N side as seen in Figure (4.2), we continued our calculations in the S (Superconducting) side, where the order parameters are not equal to zero.

In the Superconducting (S) region as seeing in Figure (4.3), the BdG Hamiltonian is showing in the Equation (4.14).

$$\begin{pmatrix} -\frac{\hbar^2}{2m} \frac{\partial^2}{\partial x^2} - \varepsilon_{Fn} & \Delta_0 e^{i\varphi} \\ \Delta_0 e^{-i\varphi} & +\frac{\hbar^2}{2m} \frac{\partial^2}{\partial x^2} + \varepsilon_{Fn} \end{pmatrix} \begin{pmatrix} u(x) \\ v(x) \end{pmatrix} = E \begin{pmatrix} u(x) \\ v(x) \end{pmatrix} \quad (4.14)$$

In here, two situations have occurred. One is the Supra-gap solutions ( $E > \Delta_0$ ). Supra-gap solution means the incident electron has more energy than the gap energy. Therefore the electron wave expected to be propagate.

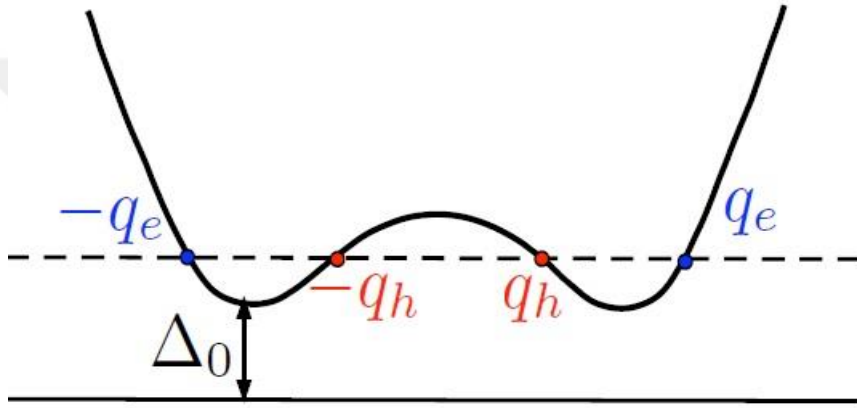


**Figure 4.3:** Superconducting (S) side spectrum [9].

The Supra-Gap solutions are stated in the equations below. In here, we have two particle-like and two hole-like solutions stated in the Equations (4.15) and (4.16) respectively [10].

$$\Psi_{\pm}^e(x) = \begin{pmatrix} u_0 e^{i\varphi/2} \\ v_0 e^{-i\varphi/2} \end{pmatrix} e^{\pm i q_e x} \quad (4.15)$$

$$\Psi_{\pm}^h(x) = \begin{pmatrix} v_0 e^{i\varphi/2} \\ u_0 e^{-i\varphi/2} \end{pmatrix} e^{\pm i q_h x} \quad (4.16)$$

Where

$$q_e = k_{Fn} \sqrt{1 + \sqrt{\frac{E^2 - \Delta_0^2}{\varepsilon_{Fn}^2}}} \quad (4.17)$$

$$q_h = k_{Fn} \sqrt{1 - \sqrt{\frac{E^2 - \Delta_0^2}{\varepsilon_{Fn}^2}}} \quad (4.18)$$

And

$$k_{Fn} = \frac{\sqrt{2m\varepsilon_{Fn}}}{\hbar} \quad (4.19)$$

Here the quantities  $u_0$  and  $v_0$  are called as quasi-particles related with electron-like and hole-like particles. The solution of the Hamiltonian gives the quasi particle results stated in the Equations (4.20) and (4.21).

$$u_0 = \sqrt{\frac{1}{2} \left( 1 + \sqrt{1 - \left( \frac{\Delta_0}{E} \right)^2} \right)} \equiv \sqrt{\frac{\Delta_0}{2E}} e^{\frac{1}{2} \operatorname{arccosh} \frac{E}{\Delta_0}} \quad (4.20)$$

$$v_0 = \sqrt{\frac{1}{2} \left( 1 - \sqrt{1 - \left( \frac{\Delta_0}{E} \right)^2} \right)} \equiv \sqrt{\frac{\Delta_0}{2E}} e^{-\frac{1}{2} \operatorname{arccosh} \frac{E}{\Delta_0}} \quad (4.21)$$

We can write the quasi-particle equations in the Wavefunction stated in the Equations (4.15) and (4.16) and we get the new wavefunction equations stated in the Equations (4.22) and (4.23).

$$\Psi_{\pm}^e(x) = \sqrt{\frac{\Delta_0}{2E}} \begin{pmatrix} e^{\frac{1}{2} \operatorname{arccosh} \frac{E}{\Delta_0}} e^{i\phi/2} \\ e^{-\frac{1}{2} \operatorname{arccosh} \frac{E}{\Delta_0}} e^{-i\phi/2} \end{pmatrix} e^{\pm iq_e x} \quad (4.22)$$

$$\Psi_{\pm}^h(x) = \sqrt{\frac{\Delta_0}{2E}} \begin{pmatrix} e^{-\frac{1}{2} \operatorname{arccosh} \frac{E}{\Delta_0}} e^{i\phi/2} \\ e^{\frac{1}{2} \operatorname{arccosh} \frac{E}{\Delta_0}} e^{-i\phi/2} \end{pmatrix} e^{\pm iq_h x} \quad (4.23)$$

Up to here, we solved the Supra-gap solutions for the S side. Let's look for Sub-gap solutions ( $E < \Delta_0$ ). In this part situation, the incident electron coming with less energy than the gap energy. Therefore, the wave expected to be evanescent.

In the sub-gap solution, the wave-vectors have an imaginary part. The real parts are remaining to the order of  $k_{Fn}$ . The analytical continuation solution is giving in the Equations (4.24) and (4.25) stated in the below.

$$q_e = k_{Fn} \sqrt{1 + i \sqrt{\frac{\Delta_0^2 - E^2}{\varepsilon_{Fn}^2}}} \quad (4.24)$$

$$q_h = k_{Fn} \sqrt{1 - i \sqrt{\frac{\Delta_0^2 - E^2}{\varepsilon_{Fn}^2}}} \quad (4.25)$$

The analytical continuation of the Equations (4.20) and (4.21) can be written similarly and stated in the Equations (4.26) and (4.27).

$$u_0 = \sqrt{\frac{\Delta_0}{2E}} e^{i \frac{\arccos \frac{E}{\Delta_0}}{2}} \quad (4.26)$$

$$v_0 = \sqrt{\frac{\Delta_0}{2E}} e^{-i \frac{\arccos \frac{E}{\Delta_0}}{2}} \quad (4.27)$$

For the evanescent waves the summation of absolute squares of quasi-particle states are not equal to zero.

$$|u_0|^2 + |v_0|^2 \neq 1 \quad (4.28)$$

On the other hand, with non-absolute summation:

$$\begin{aligned} u_0^2 + v_0^2 &= \sqrt{\frac{\Delta_0}{2E}} \left( e^{i \frac{\arccos \frac{E}{\Delta_0}}{2}} + e^{-i \frac{\arccos \frac{E}{\Delta_0}}{2}} \right) = \\ &= \frac{\Delta_0}{2E} 2 \cos\left(\frac{\arccos \frac{E}{\Delta_0}}{2}\right) = 1 \end{aligned} \quad (4.29)$$

Such this continuation is generally not unitary. Unitarity only comes from the propagating modes. The evanescent waves are complex and carry no current. Unitarity is related with the conservation of current therefore the unitarity is a confirmation in propagating modes.

In the last part, we looked for the conditions at the boundary where the Dirac barrier exist.

$$-\frac{\hbar^2}{2m} \frac{\partial^2 u}{\partial x^2} - \varepsilon_{Fn} u(x) + \Lambda \delta(x) u(x) + \Delta(x) v(x) = E u(x) \quad (4.30)$$

With integrating the Equation (4.30), the Schrödinger's boundary conditions obtained around  $x = 0$  seen in the Equations (4.31) and (4.32).



$$\partial_x u(0^+) - \partial_x u(0^-) = \frac{2m\Lambda}{\hbar^2} u(0) \quad (4.31)$$

$$\partial_x v(0^+) - \partial_x v(0^-) = \frac{2m\Lambda}{\hbar^2} v(0) \quad (4.32)$$

With approaching infinitesimal to the origin from both right-hand side and left-hand side and integrating gives the results showing above.

## 4.2. Scattering Matrix Coefficient

In this part, we want to calculate the Scattering Matrix coefficient. Firstly, we need to consider an incident electron sending from the N (left) side of the model. The incident electron wavefunction is stated in the Equation (4.33).

$$\Psi_{in}(x) = \frac{1}{\sqrt{2\pi\hbar v_e}} \begin{pmatrix} 1 \\ 0 \end{pmatrix} e^{+ik_e x} \quad (4.33)$$

The reflected particles are considered as left-moving electron or a left-moving hole. Therefore, we can write the reflection wavefunction in the Equation (4.34).

$$\Psi_{ref}(x) = \frac{r_{ee}}{\sqrt{2\pi\hbar v_e}} \begin{pmatrix} 1 \\ 0 \end{pmatrix} e^{-ik_e x} + \frac{r_{he}}{\sqrt{2\pi\hbar v_h}} \begin{pmatrix} 0 \\ 1 \end{pmatrix} e^{+ik_h x} \quad (4.34)$$

On the other hand, the transmitted particles written as right-moving electron-like or hole-like particles. The transmission wavefunction is stated in the Equation (4.35).

$$\Psi_{trans}(x) = \frac{t_{ee}}{\sqrt{2\pi\hbar w_e}} \begin{pmatrix} u_0 e^{i\varphi/2} \\ v_0 e^{-i\varphi/2} \end{pmatrix} e^{iq_e x} + \frac{t_{he}}{\sqrt{2\pi\hbar w_h}} \begin{pmatrix} v_0 e^{i\varphi/2} \\ u_0 e^{-i\varphi/2} \end{pmatrix} e^{-iq_h x} \quad (4.35)$$

The  $r_{ee}$  refers to reflection coefficient from electron to electron,  $r_{he}$  refers to reflection coefficient from electron to hole,  $t_{ee}$  refers to transmission coefficient from electron to electron and the last one  $t_{he}$  refers to transmission coefficient from electron to hole.

The wavefunctions are normalized with their velocities. The velocities are different from electron to holes and from normal to superconducting side. With normalization, same amount of flux of quasiparticle probability current carried by wavefunctions. The ‘‘r’’ and ‘‘t’’ coefficients describe a unitary matrix. Now, for the conversation of quasiparticle probability current we need to write the parameters [11].

In the N side,

$$E = \frac{\hbar^2 k_e^2}{2m} - \varepsilon_{Fn} \rightarrow v_e = \frac{1}{\hbar} \left| \frac{dE}{dk_e} \right| = \frac{\hbar k_e}{m} \quad (4.36)$$

$$E = -\frac{\hbar^2 k_h^2}{2m} + \varepsilon_{Fn} \rightarrow v_h = \frac{1}{\hbar} \left| \frac{dE}{dk_h} \right| = \frac{\hbar k_h}{m} \quad (4.37)$$

In the S side,

$$E = \sqrt{\left( \frac{\hbar^2 q_e^2}{2m} - \varepsilon_{Fn} \right)^2 + \Delta_0^2} \rightarrow w_e = \frac{1}{\hbar} \left| \frac{dE}{dq_e} \right| = \frac{\hbar q_e}{m} \quad (4.38)$$

$$E = \sqrt{\left( -\frac{\hbar^2 q_h^2}{2m} + \varepsilon_{Fn} \right)^2 + \Delta_0^2} \rightarrow w_h = \frac{1}{\hbar} \left| \frac{dE}{dq_h} \right| = \frac{\hbar q_h}{m} \quad (4.39)$$

With using the derivations stated below, we calculate the velocities showing in the Equations (4.40) and (4.41).

$$v_{e/h} = \frac{\hbar k_{e/h}}{m} \quad (4.40)$$

$$w_{e/h} = \frac{\sqrt{E^2 - \Delta_0^2}}{E} v_{e/h} = (u_0^2 - v_0^2) v_{e/h} \quad (4.41)$$

The electron and hole have different signs in the momenta in reflected wave and transmitted waves according to description.

To find the full solution, we need to apply boundary conditions stated in the below. The boundary conditions coming from the continuity are stated in the Equations (4.42) and (4.43).

$$u(0^+) = u(0^-) \quad (4.42)$$

$$v(0^+) = v(0^-) \quad (4.43)$$

The derivative boundary conditions derived from the integration of the Schrödinger's equation are stated in the Equations (4.44) and (4.45).

$$\partial_x u(0^+) - \partial_x u(0^-) = \frac{2m\Lambda}{\hbar^2} u(0) \quad (4.44)$$

$$\partial_x v(0^+) - \partial_x v(0^-) = \frac{2m\Lambda}{\hbar^2} v(0) \quad (4.45)$$

The four boundary conditions created four linear equations to find four unknowns  $r_{ee}$ ,  $r_{he}$ ,  $t_{ee}$  and  $t_{he}$ .

### 4.3. Solution of the Andreev Approximation

The Andreev approximation states that in the low energies fermi approximation can be made. This approximation makes the equation sets very simple. This approximation is using also in classical BTK model. After the derivation of the classical results, we showed our non-fermi approximation solutions and the purpose of this thesis in the Chapter 5.

$$E, \Delta_0 \ll \varepsilon_{Fn} \quad (4.46)$$

The approximation made in the Equation (4.46) refers to the approximations stated in the equations below.

$$k_{e/h} \approx q_{e/h} \approx k_{Fn} \quad (4.47)$$

And

$$v_{e/h} \approx v_{Fn} \quad (4.48)$$

$$w_{e/h} \approx \frac{\sqrt{E^2 - \Delta_0^2}}{E} v_{Fn} = (u_0^2 - v_0^2) v_{Fn} \quad (4.49)$$

The fermi velocity is also defined as

$$v_{Fn} = \frac{\hbar k_{Fn}}{m} \quad (4.50)$$

After the approximation, the equations of the model is solving using the boundary conditions. The results of coefficients for classical BTK model stated in the below.

$$r_{he} = \frac{u_0 v_0}{u_0^2 + Z^2 (u_0^2 - v_0^2)} e^{-i\varphi} \quad (4.51)$$

$$r_{ee} = \frac{(Z^2 + iZ)(u_0^2 - v_0^2)}{u_0^2 + Z^2 (u_0^2 - v_0^2)} \quad (4.52)$$

$$t_{ee} = \frac{(1 - iZ)u_0 \sqrt{u_0^2 - v_0^2}}{u_0^2 + Z^2 (u_0^2 - v_0^2)} e^{-i\varphi/2} \quad (4.53)$$

$$t_{he} = \frac{(iZ)v_0\sqrt{u_0^2 - v_0^2}}{u_0^2 + Z^2(u_0^2 - v_0^2)} e^{-i\phi/2} \quad (4.54)$$

And

$$Z = \frac{\Lambda m}{\hbar^2 k_{Fn}} = \frac{\Lambda}{\hbar v_{Fn}} \quad (4.55)$$

The  $Z$  is the dimensionless parameter of the transparency of the interface in BTK model. If  $Z$  is very small from one the solution called very transparent interface. On the other side, if  $Z$  is greater than one the solution called weakly transparent interface. Transparency is referred as transmission probability  $T_N$  of the junction in the normal case. If the gap in superconducting side is goes to zero of the temperature decreased below critical temperature, The BTK transmission probability goes as  $T_N$ .

$$T_N = \frac{1}{1 + Z^2} \quad (4.56)$$

Transmission and reflection coefficients can be written as a different notation using in the equations below [12].

$$A \doteq A_{LL}^{he} \doteq |r_{he}|^2 \quad (4.57)$$

$$B \doteq A_{LL}^{ee} \doteq |r_{ee}|^2 \quad (4.58)$$

$$C \doteq A_{RL}^{ee} \doteq |t_{ee}|^2 \quad (4.59)$$

$$D \doteq A_{RL}^{he} \doteq |t_{he}|^2 \quad (4.60)$$

Now we can look for the solutions for Supra-gap and sub-gap.

For Supra-gap ( $E > \Delta_0$ ),

$$A(E) = \frac{\Delta_0^2}{\left(E + (1 + 2Z^2)\sqrt{E^2 - \Delta_0^2}\right)^2} \quad (4.61)$$

$$B(E) = \frac{4Z^2(1 + 2Z^2)(E^2 - \Delta_0^2)}{\left(E + (1 + 2Z^2)\sqrt{E^2 - \Delta_0^2}\right)^2} \quad (4.62)$$

$$C(E) = \frac{2(1+2Z^2)(E^2 - \Delta_0^2)(E + \sqrt{E^2 - \Delta_0^2})}{\left(E + (1+2Z^2)\sqrt{E^2 - \Delta_0^2}\right)^2} \quad (4.63)$$

$$D(E) = \frac{2Z^2\sqrt{E^2 - \Delta_0^2}(E - \sqrt{E^2 - \Delta_0^2})}{\left(E + (1+2Z^2)\sqrt{E^2 - \Delta_0^2}\right)^2} \quad (4.64)$$

The summation of the probability functions gives one (A+B+C+D=1) as required by unitarity of the S-matrix.

For Sub-gap ( $E < \Delta_0$ ),

$$A(E) = \frac{\Delta_0^2}{E^2 + (1+2Z^2)(\Delta_0^2 - E^2)} \quad (4.65)$$

$$B(E) = \frac{4Z^2(1+2Z^2)(\Delta_0^2 - E^2)}{E^2 + (1+2Z^2)(\Delta_0^2 - E^2)} \quad (4.66)$$

$$C(E) = 0 \quad (4.67)$$

$$D(E) = 0 \quad (4.68)$$

In the sub-gap case the transmission coefficients go to zero. Also, if we look at the condition that  $E = \Delta_0$ , the supra-gap transmission coefficients also goes to zero which means no propagation waves among the superconducting side. Therefore, we can also easily verify that for zero transmission coefficients the summation condition gives one (A+B=1).

#### 4.4. Andreev Reflection

##### 4.4.1. The ideal interface

The ideal interface is the condition of  $Z = 0$  where no barrier in the junction. In this section we tried to analyze the ideal case. In here, the Andreev-reflection amplitude for electron to hole conversion coefficient stated in Equation (4.69) and hole to electron coefficient stated in Equation (4.70).

$$r_{he} = \frac{u_0}{v_0} e^{-i\varphi} = e^{-i\varphi} \left\{ \begin{array}{l} e^{-i\arccos\frac{E}{\Delta_0}} \rightarrow E < \Delta_0 \\ e^{-\operatorname{arccosh}\frac{E}{\Delta_0}} \rightarrow E > \Delta_0 \end{array} \right\} \quad (4.69)$$

$$r_{eh} = \frac{v_0}{u_0} e^{i\varphi} = e^{i\varphi} \begin{cases} e^{-i \arccos \frac{E}{\Delta_0}} \rightarrow E < \Delta_0 \\ e^{-\operatorname{arccosh} \frac{E}{\Delta_0}} \rightarrow E > \Delta_0 \end{cases} \quad (4.70)$$

The coefficients behavior is shown in the Figure (4.4).

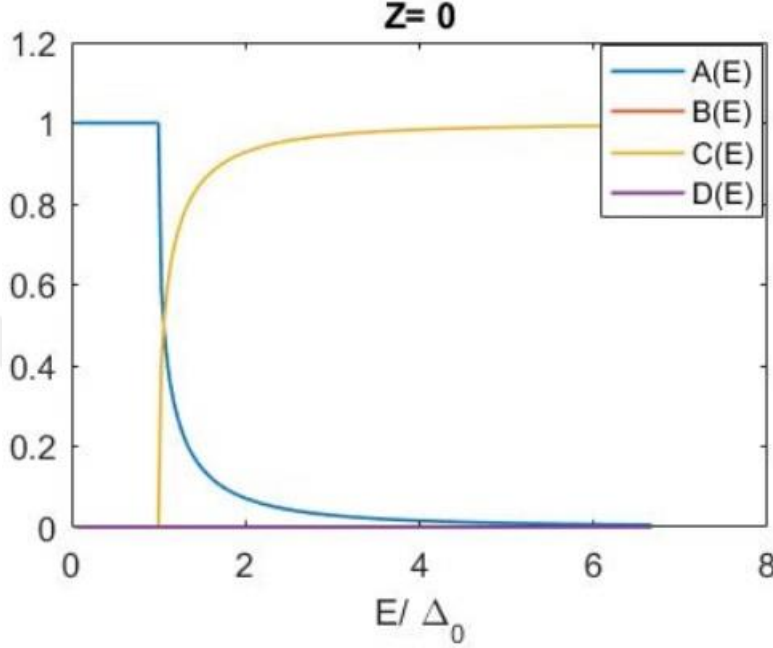


**Figure 4.4:** The probability coefficients in BTK model for  $Z=0$ .

As seeing in the Figure (4.4) the coefficients B and D are vanishing.

For sub-gap regime ( $E < \Delta_0$ )

$$A(E) = 1 \quad (4.71)$$

$$B(E) = 0 \quad (4.72)$$

$$C(E) = 0 \quad (4.73)$$

$$D(E) = 0 \quad (4.74)$$

In here A is the Andreev reflection coefficient, B is normal reflection coefficient, C is electron-like particle transmission coefficient and D is hole-like particle transmission coefficient. In the sub-gap regime, we can see that for an ideal interface all the incident electron reflected as a hole. Therefore, we see only Andreev reflection in this model. This situation is called as Andreev reflection [13-14]. The momentum is not conserved

but the charge is conserved. Because of the fermi approximation, we can say this the momentum is almost conserved.

For supra-gap regime ( $E < \Delta_0$ )

$$A(E) = \frac{\Delta_0^2}{\left(E + \sqrt{E^2 - \Delta_0^2}\right)^2} \quad (4.75)$$

$$B(E) = 0 \quad (4.76)$$

$$C(E) = \frac{2\sqrt{E^2 - \Delta_0^2}}{\left(E + \sqrt{E^2 - \Delta_0^2}\right)} \quad (4.77)$$

$$D(E) = 0 \quad (4.78)$$

For energies above the gap, electron transmission probability gets finite values. Increasing the energy will result to full transmission on the superconducting side. For supra-gap regime the particle probability is divided into Andreev reflection and electron-like transmission coefficients.

#### 4.4.2. Interface with arbitrary transparency

In this section, we look for non-ideal cases ( $Z > 0$ ). In this interface, still a probability exists for the electrons reflection as hole. On the other hand, changing the barrier strength also results to normal reflection. Therefore, with creating a potential barrier in the junction results for both Andreev and normal reflection. In the Figure 4.5 we can see that as we increase the barrier the particle most likely reflect as electron (normal reflection). On the other hand, we can see that clearly when the energy equals to the gap, the particle most likely reflected as hole (Andreev reflection). The electron-like transmission coefficient ( $C(E)$ ) is decreasing with increasing barrier strength. Also, we can see that there is a small amount of increment seeing in the hole-like transmission coefficient with increasing barrier strength. The calculation of the coefficients was done with using computational programming. With using our algorithm, we got the same results as originally Blonder-Tinkham-Klapwijk model. As we can see in the Figure (4.5), Andreev reflection coefficient act as Dirac-Delta function as the barrier strength increases. On the other hand, normal reflection and e-like Transmission coefficients getting increase.

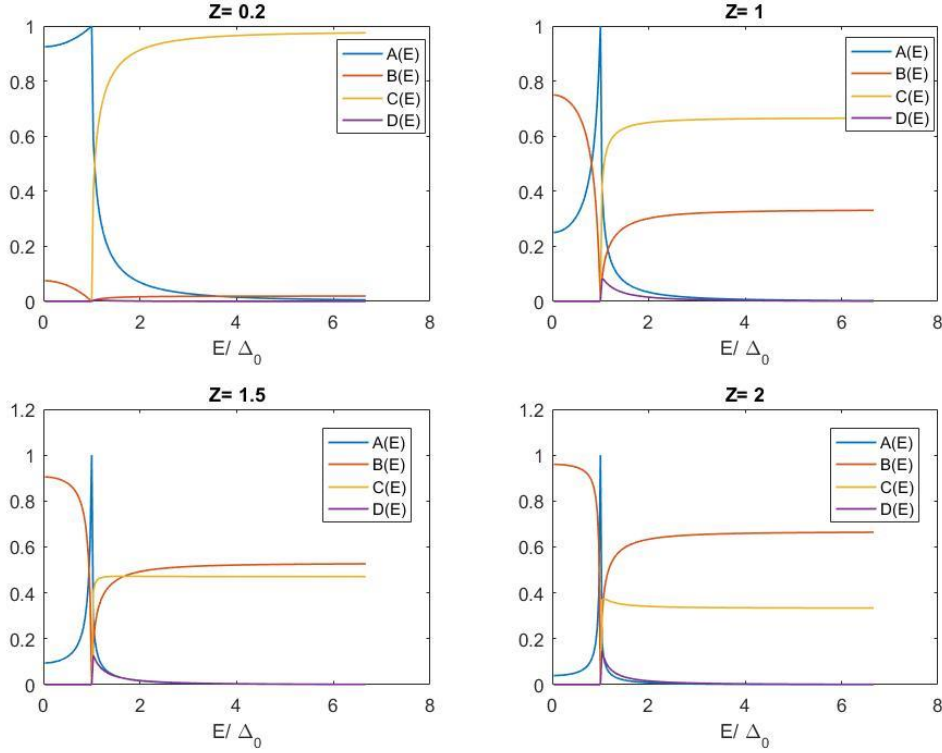


**Figure 4.5:** Reflection and transmission coefficients with increasing barrier strength.

#### 4.5. Current and Conductance

The current transport through the single channel system is expressed by Landauer-Büttiker expression seeing in the Equation (4.79) [16].

$$I = \frac{2e^2}{h} \int dE T(E) (f_L(E) - f_R(E)) \quad (4.79)$$

$$T(E) = 1 - R(E) \quad (4.80)$$

In here  $T(E)$  is the transmission coefficient and  $R(E)$  is the reflection coefficient. The “2” factor coming from spin degeneracy and  $f_{L,R}$  functions are fermi distribution functions for left hand and right hand side particles.

$$f_{L/R}(E) = \frac{1}{1 + e^{(E - \mu_{L/R})/k_B T}} \quad (4.81)$$

In our model for a single channel, the sample is contacted with one normal and one superconducting electrode. Therefore, the Landauer-Büttiker formalism is forming as stated in the Equation (4.82).



$$I = \frac{2e^2}{h} \int dE(1 - B(E) + A(E))(f_L(E) - f_R(E)) \quad (4.82)$$

In here, again  $B(E)$  is the normal reflection and  $A(E)$  is the Andreev reflection. The main logic in here, normal reflection decreases the current on the other hand Andreev reflection increases the current.

The theoretical approach allows us to investigate the results as zero temperature. The Landauer-Büttiker formalism in zero temperature is seen in the Equation (4.83).

$$I = \frac{2e^2}{h} \int_0^{eV} dE(1 - B(E) + A(E)) \quad (4.83)$$

As we can see, the fermi distribution functions disappear in the zero-temperature limit. The chemical potentials are stated in the below.

$$\mu_L = \varepsilon_F + eV \rightarrow \mu_R = \varepsilon_F \rightarrow V > 0 \quad (4.84)$$

We can derive the non-linear conductance at zero temperature from here.

$$\sigma_{NS}(V) = \frac{dI}{dV} = \frac{2e^2}{h} (1 - B(eV) + A(eV)) \quad (4.85)$$

With using the conductance, we derived the Figure (4.6) showing below

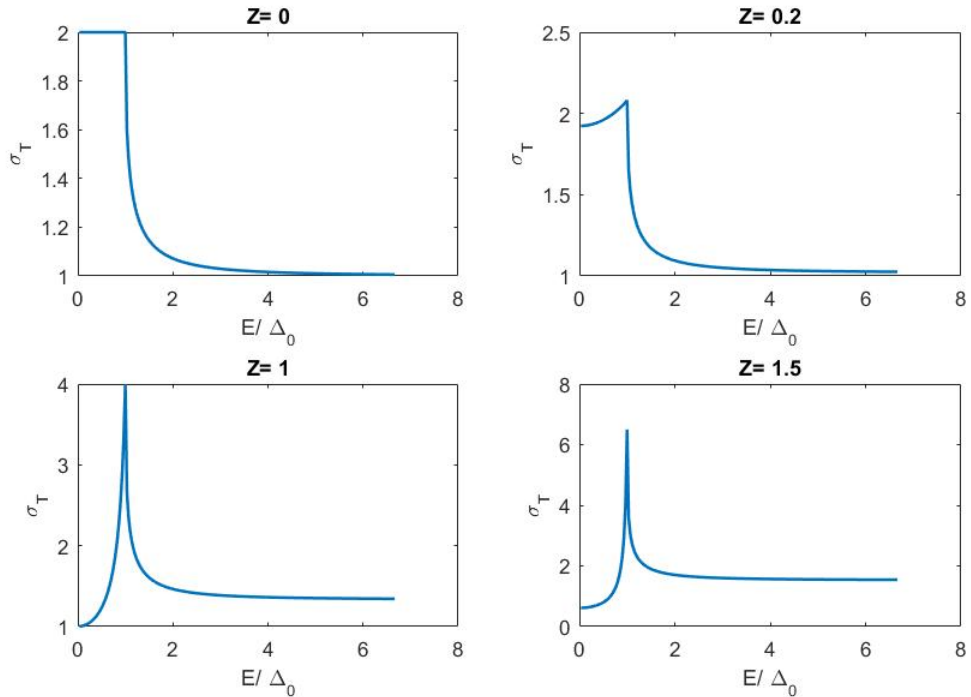


**Figure 4.6:** Changing of conductance with respect to changing energy and the barrier strength.



## 5. EFFECTS OF NEGLECTED TERMS IN JOSEPHSON JUNCTIONS

The main reason of this thesis is the understanding of the effects of neglected terms on conductance in different Josephson Junctions. Up to this chapter, we saw classical BTK model solutions [10], Andreev reflection solutions and classical conductance calculations. The idea is coming from the remove the fermi approach from the BTK model. The model we tried to solve is seen in the Figure (5.1) below.

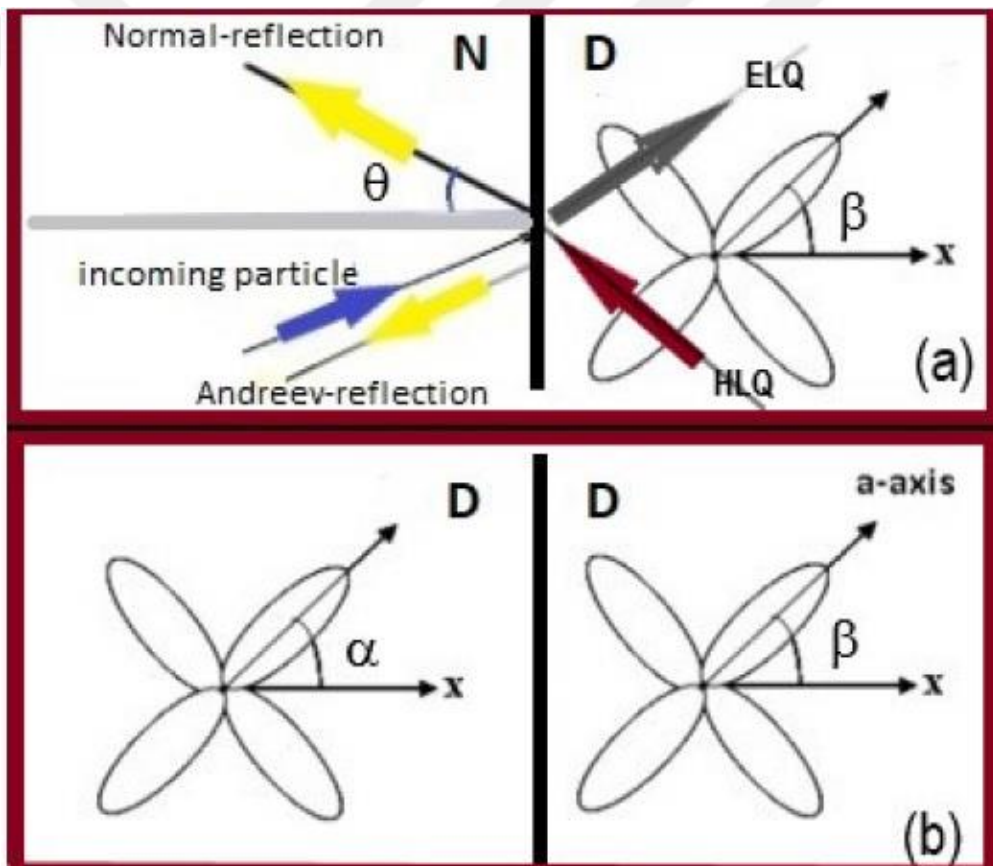


**Figure 5.1:** The basic model of ND and DD junctions. Electron and hole reflection and transmission directions are shown.

Let us consider a Josephson junction with a cuprate superconductor. We will use the standard simplified model of such a system [20], that is, assume a cylindrical Fermi surface and the order parameter stated in Equation (5.1).

$$\Delta(\theta) = \Delta_0 \cos(2(\theta - \beta)) \quad (5.1)$$

Here beta is the angle between the interface normal and the lobe direction of the order parameter. This superconductor forms one of the banks of a junction. The other one can be formed either by a similar superconductor (DD junction), or a normal conductor (ND junction).

Following the Ref. [20], we consider the junction in the x-y plane, with a Dirac functional interface potential at x equals to zero. The Fermi wave number ( $k_F$ ) and the effective mass “m” are assumed to be equal in both sides. Due to the translation invariance in y-direction, we can write the wave functions in each side in the equations below respectively [27].

$$\psi_L(r) = \psi_L(x, \theta) e^{ik_y y} \quad (5.2)$$

$$\psi_R(r) = \psi_R(x, \theta) e^{ik_y y} \quad (5.3)$$

The corresponding wavefunctions are;

$$\psi_L(x, \theta) = e^{ik_{1,x}x} (u^L, v^L \eta^L)^T + a e^{ik_{2,x}x} (v^L, u^L \eta^L)^T + b e^{-ik_{1,x}x} (u^L, v^L \eta^L)^T \quad (5.4)$$

$$\psi_R(x, \theta) = c e^{iq_{1,x}x} (u^R, v^R \eta^R)^T + d e^{-iq_{2,x}x} (v^R, u^R \eta^R)^T \quad (5.5)$$

The corresponding wavevectors are stated between Equations (5.6) and (5.7) seeing in below.

$$k_{(1)} = \sqrt{\frac{2m}{\hbar^2}} \sqrt{\sqrt{E^2 - (\Delta^L)^2} \pm E_F} \quad (5.6)$$

$$q_{(1)} = \sqrt{\frac{2m}{\hbar^2}} \sqrt{\sqrt{E^2 - (\Delta^R)^2} \pm E_F} \quad (5.7)$$

The in-plane wave vectors are stated in the Equations (5.8) and (5.9).

$$k_{ix} = k_i \cos(\theta) \quad (5.8)$$

$$q_{ix} = q_i \cos(\theta) \quad (5.9)$$

The quasi-particle derivations are stated in the Equations (5.10) and (5.11).

$$u^{L(R)} = \sqrt{\frac{1}{2} \left( 1 + \sqrt{1 - \left( \frac{\Delta^{L(R)}}{E} \right)^2} \right)} \quad (5.10)$$

$$v^{L(R)} = \sqrt{\frac{1}{2} \left( 1 - \sqrt{1 - \left( \frac{\Delta^{L(R)}}{E} \right)^2} \right)} \quad (5.11)$$

The phase of the delta function is stated in the Equation (5.12).

$$\eta^{L(R)} = e^{-i\phi^{L(R)}} = \Delta^{L(R)} / |\Delta^{L(R)}| \quad (5.12)$$

To solve this model, we need to apply Schrödinger's B.C.'s first;

$$\psi_R(x=0, \theta) = \psi_L(x=0, \theta) \quad (5.13)$$

$$\frac{\partial \psi_R(x=0, \theta)}{\partial x} - \frac{\partial \psi_L(x=0, \theta)}{\partial x} = \frac{2mH}{\hbar^2} \psi_0(x=0, \theta) \quad (5.14)$$

With the B.C.'s we get the equations below:

$$u^L = av^L + bu^L = cu^R + dv^R \quad (5.15)$$

$$\eta^L v^L + a\eta^L u^L + b\eta^L v^L = c\eta^R v^R + d\eta^L u^R \quad (5.16)$$

$$cq_1 u^R - dq_2 v^R - k_1 u^L - ak_2 v^L + bk_1 u^L = \frac{2mH}{i\hbar^2} (u^L + av^L + bu^L) \quad (5.17)$$

$$\begin{aligned} & cq_1 \eta^R v^R - dq_2 \eta^R u^R - k_1 \eta^L v^L - ak_2 \eta^L u^L + bk_1 \eta^L v^L \\ & = \frac{2mH}{i\hbar^2} (\eta^L v^L + a\eta^L u^L + b\eta^L v^L) \end{aligned} \quad (5.18)$$

With using the a, b, c and d coefficient, we can use gauss elimination to find these coefficients respectively. The matrices we used in gauss elimination is stated in the equations below. For the simplicity of the numerical analysis, we used MATLAB for numerical computation and controled our results with current conservation law. The solution of the matrices gives our coefficients.

$$A = \begin{pmatrix} v^L & u^L & -u^R & -v^R \\ \eta^L u^L & \eta^L v^L & -\eta^R v^R & -\eta^R u^R \\ (-Z - k_2)v^L & (k_1 - Z)u^L & u^R q_1 & -v^R q_2 \\ (-Z - k_2)\eta^L u^L & (k_1 - Z)\eta^L v^L & \eta^R v^R q_1 & -\eta^R u^R q_2 \end{pmatrix} \quad (5.19)$$

$$M = \begin{pmatrix} -u^L \\ -\eta^L v^L \\ (Z + k_1)u^L \\ (Z + k_1)\eta^L v^L \end{pmatrix} \quad (5.20)$$

$$C = \begin{pmatrix} a \\ b \\ c \\ d \end{pmatrix} \quad (5.21)$$

The coefficients can be found from Equation (5.22) with using MATLAB seeing in below.

$$C = A^{-1}M \quad (5.22)$$

In here a, b, c and d both are functions of energy and the angle theta. Also, a, b, c and d are complex amplitudes of the Andreev reflection, normal reflection, electron-hole and hole-electron conversion respectively. In Equation (5.14) ‘‘H’’ parameter refers to amplitude of delta functional potential barrier and Z is the dimensionless barrier strength where,

$$Z = \frac{mH}{\hbar^2 k_F \cos(\theta)} \quad (5.23)$$

The probability current of both sides is given by,

$$J_{L(R)}(x=0) = hm_{L(R)}^{-1} \text{Im}[\psi_{L(R)}^\dagger(x, \theta) \partial_x \sigma_z \psi_{L(R)}(x, \theta)]_{x=0} \quad (5.24)$$

Where ‘‘m’’ is the effective mass term on left and right side,  $\sigma_z$  is the Pauli matrix. The continuity of the current at the interface requires the statement shown in the Equation (5.25).

$$J_L(x=0) = J_R(x=0) \quad (5.25)$$

Combining boundary condition defined above with current conservation law. First check for the left side current;

$$J_L(x=0) = hm_L^{-1} \text{Im} \left[ (u_L^*, v_L^* \eta_L^*) + a^* (v_L^*, u_L^* \eta_L^*) + b^* (u_L^*, v_L^* \eta_L^*) \right] \quad (5.26)$$

$$\left[ ik_{1x} (u_L, -v_L \eta_L)^T + ik_{2x} a (v_L, -u_L \eta_L)^T - ik_{1x} b (u_L, -v_L \eta_L)^T \right]$$

$$J_L(x=0) = hm_L^{-1} \text{Im} \left[ \begin{array}{l} ik_{1x} (|u^L|^2 - |v^L|^2) - ik_{2x} |a|^2 (|u^L|^2 - |v^L|^2) \\ -ik_{1x} |b|^2 (|u^L|^2 - |v^L|^2) + ik_{1x} (b^* (|u^L|^2 - |v^L|^2) - cc) \\ + ik_{1x} a^* (v^{L*} u^L - u^{L*} v^L) - ik_{2x} a^* (v^{L*} u^L - u^{L*} v^L) \\ - ia^* b k_{1x} (v^{L*} u^L - u^{L*} v^L) - ib^* a k_{2x} (v^{L*} u^L - u^{L*} v^L) \end{array} \right] \quad (5.27)$$

With continue for the right current;

$$J_R(x=0) = hm_R^{-1} \text{Im} \left[ c^*(u_R^*, v_R^* \eta_R^*) + d^*(v_R^*, u_R^* \eta_R^*) \right] \quad (5.28)$$

$$\left[ iq_{1x} c(u_R, -v_R \eta_R)^T - iq_{2x} d(v_R, -u_R \eta_R)^T \right]$$

$$J_R(x=0) = hm_R^{-1} \text{Im} \left[ iq_{1x} |c|^2 \left( |u^R|^2 - |v^R|^2 \right) + iq_{2x} |d|^2 \left( |u^R|^2 - |v^R|^2 \right) \right. \quad (5.29)$$

$$\left. + iq_{2x} c^* d (v^{R*} u^R - u^{R*} v^R) + iq_{1x} d^* c (v^{R*} u^R - u^{R*} v^R) \right]$$

Now we can write the currents with using the probability coefficients.

$$J_L(x=0) = hm_L^{-1} \left( \text{Re}(k_{1x}) \kappa_+^L - R_a - R_b - R_{ab} \right) \quad (5.30)$$

where,

$$R_a = \text{Re}(k_{2x}) |a|^2 \kappa^L \quad (5.31)$$

$$R_b = \text{Re}(k_{1x}) |b|^2 \kappa^L \quad (5.32)$$

For the right side we have

$$J_R(x=0) = hm_R^{-1} \left( R_c + R_d + R_{cd} \right) \quad (5.33)$$

where,

$$R_c = \text{Re}(q_{1x}) |c|^2 \kappa^R \quad (5.34)$$

$$R_d = \text{Re}(q_{2x}) |d|^2 \kappa^R \quad (5.35)$$

with,

$$\kappa^{L(R)} = \left( |u^{L(R)}|^2 - |v^{L(R)}|^2 \right) \quad (5.36)$$

Note that when wave vectors “k” and “q” are complex, there appear cross terms  $R_{ab}$  (5.37) and  $R_{cd}$  (5.38). The cross terms importance are showing in the current conservation law.

$$R_{ab} = \text{Re} \left[ \left( ak_{2x} - a^* k_{1x} \right) \left( u^{L*} v^L - v^{L*} u^L \right) + k_{1x} \left( b^* \left( |u^L|^2 - |v^L|^2 \right) - cc \right) \right. \quad (5.37)$$

$$\left. + b^* ak_{2x} \left( u^{L*} v^L - v^{L*} u^L \right) + a^* bk_{1x} \left( u^{L*} v^L - v^{L*} u^L \right) \right]$$

$$R_{cd} = \text{Re} \left[ q_{1x} d^* c (v^{R*} u^R - u^{R*} v^R) + q_{2x} c^* d (v^{R*} u^R - u^{R*} v^R) \right] \quad (5.38)$$

We don't use Spin-orbit coupling in these calculations. Therefore, the relative phase factor between two spin branches is equal to one.

With using the Landauer-Büttiker formalism thus we can derive the conductance with using cross terms shown in the Equation below (5.39).

$$\sigma_T(E, \theta) = T(E, \theta) = R_c(E, \theta) + R_d(E, \theta) + R_{cd}(E, \theta) \quad (5.39)$$

We know the classical conductance is related with Andreev reflection and normal reflection coefficients. In this situation, with using the cross terms, the conductance calculations changed.

### 5.1. ND Junction

The differential conductance in this case is obtained from the general formulas by setting

$$\left\{ \begin{array}{l} \Delta^L = 0 \\ u^L = 1 \\ v^L = 0 \end{array} \right\} \quad (5.40)$$

For  $x$  greater than zero we have effective pairing potentials shown in the Equation below (5.41).

$$\Delta^R = \Delta_0^R \cos(2(\theta - \beta)) \quad (5.41)$$

The differential conductance of an ND junction for a various surface alignment angles beta is shown in the Figure (5.2) and Figure (5.3). The main difference between these two figures comes from the definition of wavevectors. In Figure (5.2) the wavevectors are taken equal to fermi wavevector. On the other hand, in Figure (5.3) the wavevectors defined as in Equations (5.6) and (5.7). One can notice that the contribution of cross terms has a huge contribution in lower  $Z$  values. On the other hand, surface alignment angle gives a difference between conductance peaks.

In the ND junction, first we used our model in Blonder-Tinkham-Klapwijk model to confirmation. These crossterms are going to zero when the wavevectors approach to fermi wavevector. After the confirmation of our algorithm with BTK model. We applied the same model to ND junction to both cases either fermi approach or not. We used this model with using MATLAB.



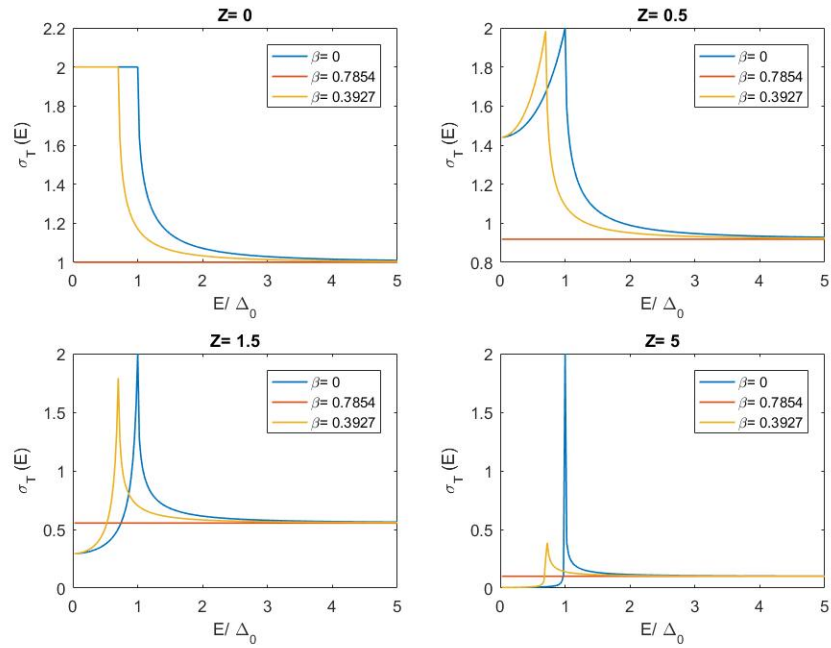


**Figure 5.2:** Conductance changing with surface alignments, barrier strength and energy with using fermi approach. Cross terms are zero.

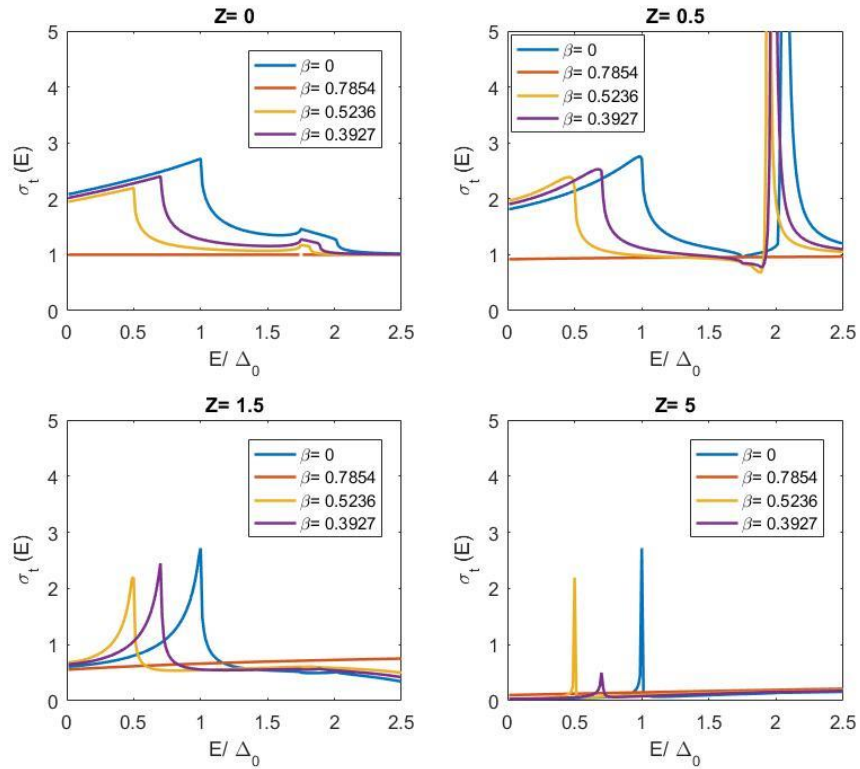


**Figure 5.3:** Conductance changing with surface alignments, barrier strength and energy without fermi approach. Cross terms are not zero.

## 5.2. DD Junction

In this model, for simplicity we choose all the material parameters of the two superconductors to be equal. The pair potentials in the left and right-side superconductors are shown in the Equations (5.42) and (5.43) respectively.

$$\Delta^L = \Delta_0^L \cos(2(\theta - \alpha)) \quad (5.42)$$

$$\Delta^R = \Delta_0^R \cos(2(\theta - \beta)) \quad (5.43)$$

The angles alpha and beta are the angles between the crystalline axis and the normal to the interface in the both side superconductors. Amplitudes of pair potentials are taken equal shown in the Equation (5.44).

$$\Delta_0^L = \Delta_0^R \quad (5.44)$$

The solutions of conductance of asymmetric contact and parallel contact are both shown in the Figures (5.4) and (5.5).

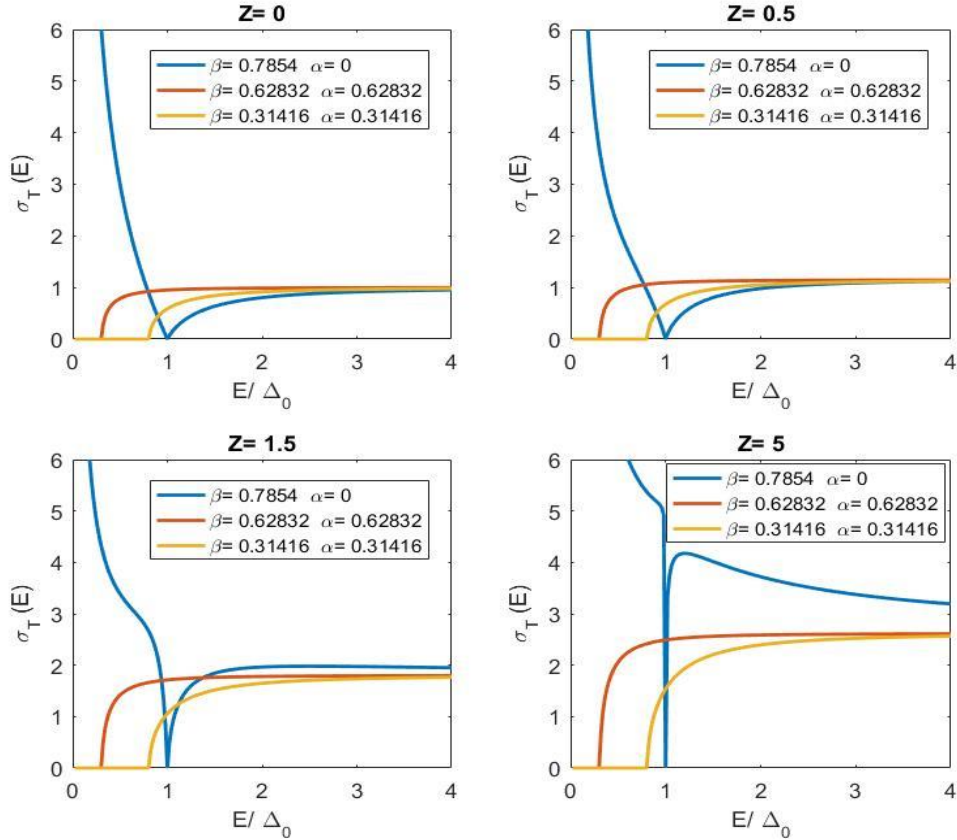


**Figure 5.4:** Conductance spectrum of two d-wave SC junction with various surface alignments for cross terms equal to zero.

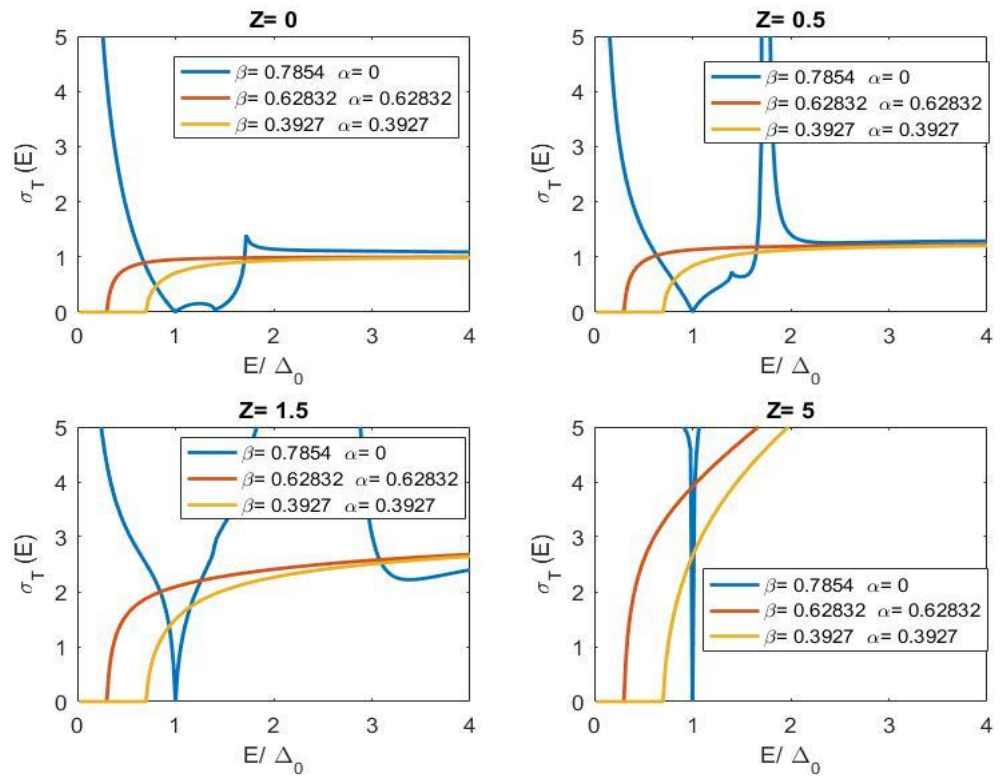


**Figure 5.5:** Conductance spectrum of two d-wave SC junction with various surface alignments for cross terms not equal to zero.

In both case where the fermi approach brings cross terms zero Figure (5.4) and non-fermi approach brings cross terms Figure (5.5) the conductance has a significant difference in small barrier strengths.



## 6. CONCLUSION

In this thesis, we tried to work on Josephson junctions which is a very popular topic. The Josephson junction phenomenon is planning to use in quantum devices and energy sectors. In the first chapters, we derived some important phenomenon about superconductivity. To understand our model, we derived the classical Andreev reflection problem. With using the calculations of the classical BTK model, we got a chance to compare our results to make correction.

We tried to solve this model without some basic approximations to show the conductance behavior which is never done before. We have shown that the differential conductance of a Josephson junction with d-wave superconductors contains contributions from the cross terms. These terms are routinely neglected, because they are zero in the limit when quasi particle wave vector amplitude is equal to fermi value. Outside of this approximation, their contribution to the differential conductance of ND and DD junctions where barrier strength changing from zero to a finite value is shown. It crucial in forming zero-bias conductance peak in DD junctions in Figure (5.4) and (5.5).

The cross-term influence is doubled the conductance peak where energy goes to two times pair potential. On the other hand, in Figure (5.5) where there is no fermi approach, we can see the conductance goes to zero where energy equals to pairing potential and one and half times greater than the pairing potential.

In ND case, the Figure (5.2) where there the cross terms are zero is shown similar behavior with classical BTK model. However, in Figure (5.3) where cross terms are not zero we can see double conductance peaks where the barrier strength smaller than one. As the barrier strength increases, the conductance behavior became like classical BTK model. In both cases, we can see the significant effects of cross terms in Josephson junctions.



## REFERENCES

- [1] **Muller, B. J.** (2010). The Development of a SQUID-based Gradiometer, Thesis MS, Stellenbosch University.
- [2] **London, F., and London, H.** (1935). The electromagnetic equations of the supraconductor, Proceedings of the Royal Society of London, A149:71-88
- [3] **Müller, K. A., and Bednorz, J. G.** (1986). Possible high  $T_c$  superconductivity in the Ba-La-Cu-O system, Zeitschrift für Physik B Condensed Matter, 64:189–193
- [4] **Kitaph, F.** (2011). Fabrication of Nanoscale Josephson Junctions and Superconducting Quantum Interference Devices, Thesis MS, University of Waterloo.
- [5] **Schmidt, V. V.** (1997). The Physics of Superconductors, Springer.
- [6] **Orlando, T. P., and Delin, K. A.** (1991) , Foundations of Applied Superconductivity, Addison-Wesley.
- [7] **Tinkham, M.** (2004). Introduction to Superconductivity, Courier Dover Publications,
- [8] **Bland, J.** (2002). A Mossbauer Spectroscopy and Magnetometry Study of Magnetic Multilayers and Oxides, Thesis MS, University of Liverpool.
- [9] **Dolcini, F.** (2009). Andreev Reflection, Lecture Notes for 23 Physics GradDays, Heidelberg.
- [10] **Blonder, G. E., Tinkham, M., Klapwijk, T. M.** (1982). Phys. Rev. B **25**, 4515.
- [11] **Beenakker, C. W. J.** (1992). *Transport Phenomena in Mesoscopic Systems* (eds. H. Fukuyama, and T. Ando), Springer Series in Solid State Science **109**, Springer Verlag Heidelberg.
- [12] **Lambert, C. J., Raimondi, R.** (1998). J. Phys. Cond. Matt. **10**, 901; **Lambert, C. J.** (1991). J. Phys. Cond. Matt. **3**, 6579
- [13] **Andreev, A. F.** (1964). Sov. Phys. JETP **19**, 1228.
- [14] **Artemenko, S. N., Volkov, A. F., and Zaitsev, A. V.,** JETP Lett. **28**, 589 (1978); Sov. Phys. JETP **49**, 924 (1979); Solid State Comm. **30**, 771 (1979).
- [15] **Zagoskin, A. M.** (1998). Quantum Theory of Many-Body System, Springer Verlag New York.
- [16] **Blanter, Y., Büttiker, M.** Shot-Noise in Mesoscopic Conductors, [ArXiv version cond-mat/9910158].
- [17] **Bardeen, J., Cooper, L. N., and Schrieffer, J. R.** (1957). Phys. Rev. **108**, 1175.
- [18] **Scalapino, D. J.** (1995) Phys. Rep. **250**, 329.

- [19] **Bardeen, J.** (1961). Phys. Rev. Lett. **6**, 57.
- [20] **Kashiwaya, S., and Tanaka, Y.** (2000). Rep. Prog. Phys. **63**, 1641
- [21] **Furusaki, A.** (1999). Superlattices Microstruct. **25**, 809.
- [22] **de Gennes, P. G., and Saint-James, D.** (1963). Phys. Lett. **4**, 151
- [23] **Clarke, J., and Braginski, A. I.** (2006). The SQUID Handbook, vol. **2**, Wiley.
- [24] **Cooper, L. N.** (1956). Bound Electron Pairs in a Degenerate Fermi Gas, Phys. Rev., **104**, pp. 1180-1190.
- [25] **Bardeen, J.** (1963). Tunneling into Superconductors, Phys. Rev. Lett., **9**, pp. 140-150.
- [26] **Josephson, B. D.** (1962). Possible New Effects in Superconductive Tunneling, Phys. Lett., **1**, pp. 250-253.
- [27] **Kittel, C.** (2004). Introduction to Solid State Physics, Wiley.



## **CURRICULUM VITAE**

**Name Surname:** Denizhan Ekin ÖNDER

**Place and Date of Birth:** Ankara, 17.11.1992

**E-Mail:** d.ekinonder@gmail.com

### **EDUCATION:**

**B.Sc.:** 2016, ITU, Faculty of Literature and Science, Physics Engineering